Boudias, C. & Monceau, D. (1989). *CaRIne Cristallographie*. Version 3.0. Distributed by Divergent S. A., Rond Point Guy Denielou, Centre de Transfert, 60200 Compiegne, France.
Fraker, A. C. & Stadelmaier, H. H. (1969). *Trans. Metall. Soc. AIME*, **237**, 847–850.
Herle, P. S., Vasanthacharya, N. Y., Hegde, M. S. & Gopalakrishnan, J. (1995). *J. Alloys Compd.* **217**, 22–24.
Holleck, H. & Thummler, F. (1967). *Monatsh. Chem.* **98**, 133–138.
Houmes, J. D., Bem, D. S. & zur Loye, H.-C. (1993). *MRS Symposium Proceedings: Covalent Ceramics II: Non-Oxides*, Vol. 327, edited by A. R. Barron, G. S. Fischman, M. A. Fury & A. F. Hepp, pp. 153–164. Boston: Materials Research Society.
Howard, C. J. (1982). *J. Appl. Cryst.* **15**, 615–620.
Izumi, F. (1993). *The Rietveld Method*, edited by R. A. Young, ch. 13. Oxford: Oxford University Press.
Kim, Y.-I. & Izumi, F. (1994). *J. Ceram. Soc. Jpn*, **102**, 401–404.
Kislyakova, E. N. (1943). *Russ. J. Phys. Chem.* **17**, 108–112.
Mueller, M. H. & Knott, H. W. (1963). *Trans. AIME*, **227**, 674–678.
Nyman, H., Andersson, S., Hyde, B. G. & O'Keeffe, M. (1978). *J. Solid State Chem.* **26**, 123–131.
Pollock, C. B. & Stadelmaier, H. H. (1970). *Metall. Trans.* **1**, 767–770.
Rietveld, H. M. (1969). *J. Appl. Cryst.* **2**, 65–71.
Thompson, P., Cox, D. E. & Hastings, J. B. (1987). *J. Appl. Cryst.* **20**, 79–83.
Weil, K. S. & Kumta, P. N. (1997). *J. Solid State Chem.* **128**, 185–190.
Weil, K. S. & Kumta, P. N. (1996). *Mater. Sci. Eng. B*, **38**, 109–117.
Westgren, A. (1933). *Jernkontorets Ann.* **117**, 1–4.
Westgren, A. & Phragmen, G. (1928). *Trans. Am. Soc. Steel Treat.* **13**, 539–544.
Young, R. A. (1993). *The Rietveld Method*, edited by R. A. Young, ch. 1. Oxford: Oxford University Press.
Yurko, G. A., Barton, J. W. & Parr, J. G. (1959). *Acta Cryst.* **12**, 909–911.

Acta Cryst. (1997). C**53**, 1748–1751

Cerous Silver Nitrate, $Ag_6Ce(NO_3)_9$

NATHALIE AUDEBRAND, JEAN-PAUL AUFFRÉDIC, PATRICIA BÉNARD-ROCHERULLÉ AND DANIEL LOUËR

Laboratoire de Chimie du Solide et Inorganique Moléculaire, (CNRS, UMR 6511), Groupe de Cristallochimie, Université de Rennes I, Avenue du Général Leclerc, 35042 Rennes CEDEX, France. E-mail: daniel.louer@univ-rennes1.fr

(Received 16 January 1997; accepted 10 June 1997)

Abstract

The title compound was synthesized from a nitric acid solution of silver and cerium(III) nitrates at 333 K. The structure is built from irregular icosahedral $[Ce(NO_3)_6]^{3-}$ anions and Ag^+ cations. The O atoms around one of the two independent Ag atoms form a distorted bicapped trigonal prism, while a non-definite polyhedron is observed around the other. Two types of nitrate groups ensure the continuity and give a three-dimensional aspect to the crystal structure.

Comment

The present structure investigation was performed as part of a detailed study of the thermal behaviour of precursors of cerium oxide which have a high surface area, based on Ce^{III} and Ce^{IV} nitrates. Among these compounds, the cerium(III) precursors $M^I_2Ce^{III}(NO_3)_5.4H_2O$ with M = Rb (Audebrand, Auffrédic, Louër, Guillou & Louër, 1996) and NH_4 (Audebrand, Auffrédic & Louër, 1997*a*) have been thoroughly analysed. The family has been extended recently to include a mixed Ce^{III} and Ag precursor, $Ag_2Ce(H_2O)(NO_3)_5$ (Audebrand, Auffrédic & Louër, 1997*b*). In the course of this study, a new phase was observed and identified from its powder diffraction pattern. In order to determine its chemical formula, single crystals were prepared successfully from a nitric acid solution of silver and cerium(III). Although the crystals were very unstable under ambient conditions, the structure determination could be performed. The solution reported here demonstrates that this new compound is the hexasilver cerium(III) nitrate $Ag_6Ce(NO_3)_9$, which is not isostructural with the chemically related ammonium neodymium phase (Manek & Meyer, 1993).

The structure of the title compound (Fig. 1) consists of independent $[Ce(NO_3)_6]^{3-}$ anions in the form of irregular icosahedra, in which Ce atoms are linked to six nitrate groups, as reported previously for the oxonium cerium(III) nitrate hydrate (Fig. 3 in Guillou, Auffrédic, Louër & Louër, 1993). The mean Ce—O distance (2.628 Å) is in agreement with the value (2.649 Å) calculated by the bond-valence method (Brown, 1981, 1996) for Ce^{III} bonded to 12 O atoms. The $[Ce(NO_3)_6]^{3-}$ anions, centred at the origin of the cell in the 6(*b*) position of the $R\bar{3}c$ space group, fall into lines along the *c* axis with a periodicity of half the axis,

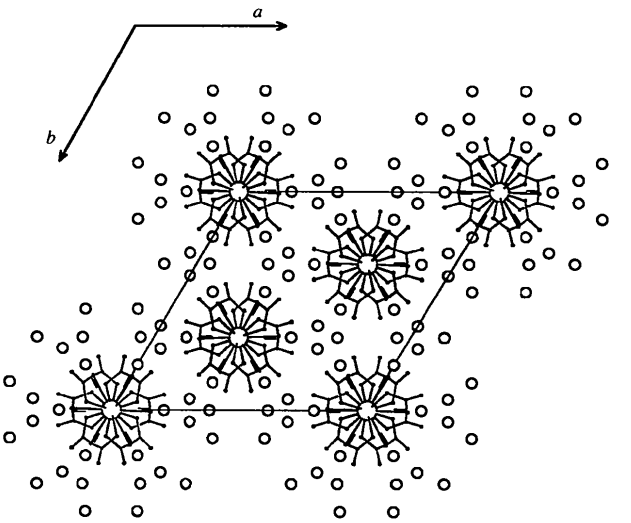

Fig. 1. Projection of the structure of $Ag_6Ce(NO_3)_9$ along the *c* axis. Large and medium circles represent Ce and Ag atoms, respectively. For clarity, nitrate groups around Ag atoms are omitted.

i.e. 7.286 Å. Each Ag^+ cation is surrounded by eight O atoms, in the form of a distorted bicapped trigonal prism in the case of Ag2 (Fig. 2) and a non-definite polyhedron for Ag1. Such a coordination number for silver has been found in the structure of $Ag(ClO_4)(H_2O)$ (Wartchow & Ludwig, 1995). The mean Ag—O distances (2.695 Å for Ag1 and 2.641 Å for Ag2) are in good agreement with the value (2.611 Å) calculated by the bond-valence method (Brown, 1981) for Ag bonded to eight O atoms. The longest Ag—O distance of 3.091 (2) Å (Ag1—O11), the shortest distance of 2.367 (5) Å (Ag1—O12), and the high isotropic displacement parameter of O11 can be explained by the rigidity of the almost perfect nitrate group induced by the special positions [18(*e*)] of Ag1, N1 and O11 (see Tables 1 and 2). Although an Ag—O distance of 3.091 (2) Å is uncommon, the largest cation–anion distance that has been considered to represent a bond is 3.15 Å for Ag—O, according to Donnay & Allmann (1970). Also, it should be noted that there is another such long distance [3.024 (47) Å] in the structure of the unstable phase of silver nitrate (Meyer, Rimsky & Chevalier, 1976).

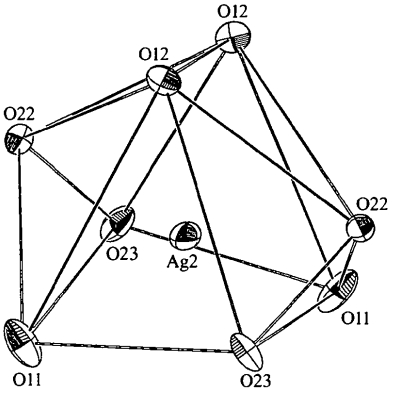

Fig. 2. View of the environment of the Ag2 atom, showing the distorted bicapped trigonal prism. Displacement ellipsoids are plotted at the 20% probability level.

The first nitrate group (N1) derives from the class V_2 proposed by Leclaire (1979); however, there are two additional Ag1—O11 bonds (Fig. 3*a*). This class is the less common and is characterized by some metal–oxygen bonds greater than 3 Å (Donnay & Allmann, 1970). The nitrate group is symmetric (see Table 2) with equal N—O distances and O—N—O angles. The second nitrate group (N2) belongs to the class III_{6b} proposed by Leclaire (Fig. 3*b*). As reported for this class, the distance from the N atom to O23 [1.221 (6) Å] is shorter than the other N—O distances (mean value 1.259 Å). The displacement parameter of atom O23 is higher than those of the other O atoms and the O21—N2—O22 angle is smaller than the O—N—O angles involving O23.

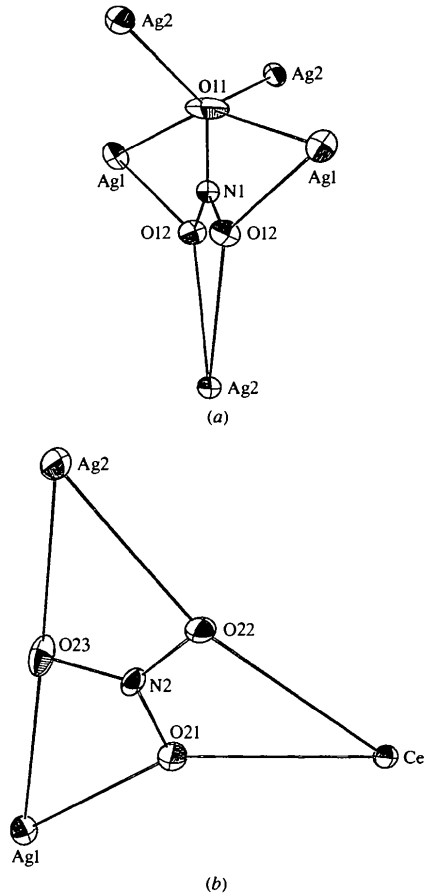

Fig. 3. View of the nitrate groups containing N1 (*a*) and N2 (*b*). Displacement ellipsoids are plotted at the 20% probability level.

The Ag atoms and the first nitrate group (N1, O11 and O12) form a honeycomb structure in the *ab* plane induced by the hexagonal symmetry, as shown in Fig. 1. The Ag1—Ag2 distance [2.933 (1) Å] is close to that between atoms in metallic silver, which is 2.899 Å (Pearson, 1966). This framework generates tunnels along the *c* axis, which are filled by the 'chains' of $[Ce(NO_3)_6]^{3-}$ anions. The second nitrate group (N2, O21, O22 and O23) ensures the connection between Ag and Ce atoms, giving a three-dimensional aspect to the crystal structure.

Experimental

A nitric acid solution of cerium(III) nitrate hexahydrate, $Ce(NO_3)_6.6H_2O$, and silver nitrate, $AgNO_3$, in the ratio 1:2, was evaporated at 333 K. Colourless hexagonal crystals of $Ag_6Ce(NO_3)_9$ were formed after two days, along with those of $Ag_2Ce(H_2O)(NO_3)_5$ (Audebrand, Auffrédic & Louër, 1997*b*).

Crystal data

$Ag_6Ce(NO_3)_9$	Mo $K\alpha$ radiation
M_r = 1345.43	λ = 0.71073 Å

Trigonal
$R\bar{3}c$
a = 16.402 (2) Å
c = 14.573 (2) Å
V = 3395.3 (7) Å^3
Z = 6
D_x = 3.948 Mg m^{-3}
D_m not measured

Cell parameters from 25 reflections
θ = 8–13°
μ = 7.195 mm^{-1}
T = 293 (2) K
Hexagonal plate
0.6 × 0.6 × 0.3 mm
Colourless

Data collection

Enraf–Nonius CAD-4 diffractometer
$\theta/2\theta$ scans
Absorption correction: empirical *via* ψscans (North, Phillips & Mathews, 1968)
T_{min} = 0.061, T_{max} = 0.115
2221 measured reflections
1104 independent reflections

961 reflections with $I > 2\sigma(I)$
R_{int} = 0.034
θ_{max} = 29.98°
$h = 0 \rightarrow 23$
$k = -23 \rightarrow 0$
$l = 0 \rightarrow 20$
3 standard reflections
frequency: 60 min
intensity decay: 1.26%

Refinement

Refinement on F^2
$R[F^2 > 2\sigma(F^2)]$ = 0.040
$wR(F^2)$ = 0.115
S = 1.006
1104 reflections
69 parameters
$w = 1/[\sigma^2(F_o^2) + (0.0664P)^2 + 75.0686P]$
where $P = (F_o^2 + 2F_c^2)/3$
$(\Delta/\sigma)_{max} < 0.001$

$\Delta\rho_{max}$ = 2.54 e Å^{-3}
$\Delta\rho_{min}$ = −1.41 e Å^{-3}
Extinction correction: *SHELXL*93 (Sheldrick, 1993)
Extinction coefficient: 0.00113 (10)
Scattering factors from *International Tables for Crystallography* (Vol. C)

Table 1. *Fractional atomic coordinates and equivalent isotropic displacement parameters (Å^2)*

$U_{eq} = (1/3)\Sigma_i\Sigma_j U^{ij} a_i^* a_j^* \mathbf{a}_i.\mathbf{a}_j$.

	x	y	z	U_{eq}
Ce	0	0	0	0.0187 (2)
Ag1	0.20633 (4)	0	1/4	0.0360 (3)
Ag2	0.38513 (4)	0	1/4	0.0421 (3)
N1	0.5664 (4)	0	1/4	0.0262 (13)
O11	0.6418 (4)	0	1/4	0.056 (2)
O12	0.8484 (3)	0.2075 (3)	0.4860 (3)	0.0340 (9)
N2	0.9512 (4)	0.8275 (3)	0.1174 (4)	0.0273 (10)
O21	0.9631 (3)	0.0822 (3)	0.1348 (3)	0.0338 (10)
O22	0.8488 (3)	0.8428 (3)	0.9492 (3)	0.0298 (9)
O23	0.9305 (4)	0.7591 (3)	0.1657 (4)	0.0461 (13)

Table 2. *Selected geometric parameters (Å, °)*

Ce—O21^{i}	2.619 (5)	Ag1—O23^{xviii}	2.854 (6)
Ce—O21^{ii}	2.619 (5)	Ag1—O23^{xix}	2.854 (6)
Ce—O21^{iii}	2.619 (5)	Ag2—O11^{xiv}	2.671 (2)
Ce—O21^{iv}	2.619 (5)	Ag2—O11^{xiii}	2.671 (2)
Ce—O21^{v}	2.619 (5)	Ag2—O12^{xx}	2.577 (5)
Ce—O21^{vi}	2.619 (5)	Ag2—O12^{xiv}	2.577 (5)
Ce—O22^{vii}	2.637 (4)	Ag2—O22^{xxi}	2.639 (4)
Ce—O22^{viii}	2.637 (4)	Ag2—O22^{xxii}	2.639 (4)
Ce—O22^{ix}	2.637 (4)	Ag2—O23^{xxiii}	2.677 (6)
Ce—O22^{x}	2.637 (4)	Ag2—O23^{xxiv}	2.677 (6)
Ce—O22^{xi}	2.637 (4)	Ag1—Ag2	2.9326 (11)
Ce—O22^{xii}	2.637 (4)	N1—O11	1.236 (10)
Ag1—O11^{xiii}	3.091 (2)	N1—O12^{xiv}	1.246 (5)
Ag1—O11^{xiv}	3.091 (2)	N1—O12^{xx}	1.246 (5)
Ag1—O12^{xv}	2.367 (5)	N2—O21^{xix}	1.269 (7)
Ag1—O12^{xvi}	2.367 (5)	N2—O22^{xxiv}	1.248 (7)
Ag1—O21^{xvii}	2.469 (5)	N2—O23	1.221 (6)
Ag1—O21^{ii}	2.469 (5)		
O11—N1—O12^{xiv}	120.4 (4)	O22^{xxiv}—N2—O21^{xix}	117.5 (5)
O11—N1—O12^{xx}	120.4 (4)	O23—N2—O21^{xix}	120.1 (6)
O12^{xiv}—N1—O12^{xx}	119.2 (7)	O23—N2—O22^{xxiv}	122.4 (6)

Symmetry codes: (i) $x-y-1, x-1, -z$; (ii) $1-x+y, 1-x, z$; (iii) $1-x, -y, -z$; (iv) $-y, x-y-1, z$; (v) $y, 1-x+y, -z$; (vi) $x-1, y, z$; (vii) $x-1, y-1, z-1$; (viii) $1-x, 1-y, 1-z$; (ix) $y-1, -x+y, 1-z$; (x) $x-y, x-1, 1-z$; (xi) $1-y, x-y, z-1$; (xii) $-x+y, 1-x, z-1$; (xiii) $x-y-\frac{1}{3}, x-\frac{2}{3}, \frac{1}{3}-z$; (xiv) $\frac{1}{3}+y, \frac{2}{3}-x+y, \frac{2}{3}-z$; (xv) $x-y-\frac{1}{3}, \frac{1}{3}-y, \frac{5}{6}-z$; (xvi) $x-\frac{2}{3}, y-\frac{1}{3}, z-\frac{1}{3}$; (xvii) $y, x-1, \frac{1}{2}-z$; (xviii) $1-x, -x+y, \frac{1}{2}-z$; (xix) $1-y, x-y, z$; (xx) $x-\frac{1}{3}, x-y-\frac{2}{3}, z-\frac{1}{6}$; (xxi) $x-\frac{1}{3}, y-\frac{2}{3}, z-\frac{2}{3}$; (xxii) $\frac{1}{3}+x-y, \frac{2}{3}-y, \frac{7}{6}-z$; (xxiii) $x-\frac{2}{3}, x-y-\frac{1}{3}, z+\frac{7}{6}-1$; (xxiv) $y-\frac{1}{3}, \frac{1}{3}-x+y, \frac{1}{3}-z$; (xxv) $1+x-y, x, 1-z$.

The crystal used for the structure analysis was mounted in a capillary containing dry oil to prevent its decomposition. Additionally, the crystal was kept fixed in the capillary by two glass rods. The dimensions of the crystal could only be estimated approximately because it was almost invisible in the oil. For this reason, and to take into account any absorption due to the oil, an empirical absorption correction (ψ scans; North, Philips & Mathews, 1968) was applied, rather than a numerical one. The low value of R_{int} for averaging 1104 duplicate intensities supports the view that this procedure has been successful. The maximum in the difference map is located 0.721 Å from Ag2 and the minimum 0.655 Å from Ag2. The structure was solved in the $R\bar{3}c$ space group by the Patterson method (Ce) and subsequent difference Fourier syntheses (all other atoms). Calculations were performed on a MicroVAX 3100 computer.

Data collection: *CAD-4 Software* (Enraf–Nonius, 1989). Cell refinement: *CAD-4 Software*. Data reduction: *MolEN* (Fair, 1990). Program(s) used to solve structure: *SHELXS*86 (Sheldrick, 1990). Program(s) used to refine structure: *SHELXL*93 (Sheldrick, 1993). Molecular graphics: *ORTEP*II (Johnson, 1976). Software used to prepare material for publication: *SHELXL*93.

Grateful thanks are expressed to the Conseil Régional de Bretagne for support to one of the authors (NA).

Supplementary data for this paper are available from the IUCr electronic archives (Reference: TA1156). Services for accessing these data are described at the back of the journal.

References

Audebrand, N., Auffrédic, J. P. & Louër, D. (1997*a*). *Thermochim. Acta*, **293**, 65–76.

Audebrand, N., Auffrédic, J. P. & Louër, D. (1997*b*). *J. Solid State Chem.* In the press.

Audebrand, N., Auffrédic, J. P., Louër, M., Guillou, N. & Louër, D. (1996). *Solid State Ionics*, **84**, 323–333.

Brown, I. D. (1981). *Structure and Bonding in Crystals*, Vol. II, edited by M. O'Keeffe & A. Navrotsky, ch. 14, pp. 1–30. London: Academic Press.

Brown, I. D. (1996). *J. Appl. Cryst.* **29**, 479–480.

Donnay, G. & Allmann, R. (1970). *Am. Mineral.* **55**, 1003–1015.

Enraf–Nonius (1989). *CAD-4 Software*. Version 5. Enraf–Nonius, Delft, The Netherlands.

Fair, C. K. (1990). *MolEN. An Interactive Intelligent System for Crystal Structure Analysis*. Enraf–Nonius, Delft, The Netherlands.

Guillou, N., Auffrédic, J. P., Louër, M. & Louër, D. (1993). *J. Solid State Chem.* **106**, 295–300.
Johnson, C. K. (1976). *ORTEP*II. Report ORNL-5138. Oak Ridge National Laboratory, Tennessee, USA.
Leclaire, A. (1979). *J. Solid State Chem.* **28**, 235–244.
Manek, E. & Meyer, G. (1993). *Z. Anorg. Allg. Chem.* **619**, 761–765.
Meyer, P., Rimsky, A. & Chevalier, R. (1976). *Acta Cryst.* B**32**, 1143–1146.
North, A. C. T., Phillips, D. C. & Mathews, F. S. (1968). *Acta Cryst.* A**24**, 351–359.
Pearson, W. B. (1966). *A Handbook of Lattice Spacings and Structures of Metals and Alloys*, Vol II, p. 80. Oxford: Pergamon Press.
Sheldrick, G. M. (1990). *Acta Cryst.* A**46**, 467–473.
Sheldrick, G. M. (1993). *SHELXL*93. *Program for the Refinement of Crystal Structures*. University of Göttingen, Germany.
Wartchow, R. & Ludwig, W. (1995). *Z. Kristallogr.* **210**, 879.

Acta Cryst. (1997). C**53**, 1751–1753

$Eu_2Si_5N_8$ and $EuYbSi_4N_7$. The First Nitridosilicates with a Divalent Rare Earth Metal

HUBERT HUPPERTZ AND WOLFGANG SCHNICK

Laboratorium für Anorganische Chemie, Universitätsstrasse 30, D-95440 Bayreuth, Germany. E-mail: wolfgang.schnick@uni-bayreuth.de

(Received 1 May 1997; accepted 13 June 1997)

Abstract

The crystal structures of dieuropium pentasiliconoctanitride, $Eu_2Si_5N_8$, and europium ytterbium tetrasiliconheptanitride, $EuYbSi_4N_7$, are based on three-dimensional networks of corner-sharing SiN_4 tetrahedra. $Eu_2Si_5N_8$ is isotypic with the previously reported Sr and Ba analogues; $EuYbSi_4N_7$ is isotypic with $SrYbSi_4N_7$ and $BaYbSi_4N_7$.

Comment

Recently, we developed a novel synthetic approach to multinary nitridosilicates by reacting alkaline earth or rare earth metals with silicon diimide in a specially developed high-frequency furnace (Huppertz & Schnick, 1997*b*). These reactions may be interpreted as the dissolution of an electropositive metal in a nitrido-analogous polymeric acid accompanied by the evolution of hydrogen.

SiO_4 and SiN_4 tetrahedra are characteristic structural elements in oxo- and nitridosilicates, respectively. These tetrahedra are commonly connected through corner sharing to give network structures. Additionally, in nitridosilicates, edge sharing has been observed ($Ba_5Si_2N_6$; Yamane & DiSalvo, 1996) as well as vertex sharing together with edge sharing of SiN_4 tetrahedra ($BaSi_7N_{10}$; Huppertz & Schnick, 1997*a*). In contrast to oxygen in oxosilicates, nitrogen in nitridosilicates shows a greater flexibility. Whereas the structural chemistry of oxosilicates is limited to terminal O atoms and simple bridging $O^{[2]}$ atoms, the nitridosilicates extend this range, exhibiting terminal $N^{[1]}$ atoms, and $N^{[2]}$, $N^{[3]}$ and $N^{[4]}$ atoms, connected to two, three and even four neighbouring Si tetrahedral centres, respectively. These structural variabilities in nitridosilicates provide a significant extension of the conventional silicate chemistry.

Until now nitridosilicates have only been obtained in combination with divalent alkaline earth metals (*e.g.* $Ca_2Si_5N_8$; Schlieper & Schnick, 1995), divalent transition metals (*e.g.* $MnSiN_2$; Maunaye, Marchand, Guyader, Laurent & Lang, 1971), or trivalent lanthanides (*e.g.* $Ce_3Si_6N_{11}$, $BaYbSi_4N_7$; Huppertz & Schnick, 1996*a*,*b*). The title compounds $Eu_2Si_5N_8$ and $EuYbSi_4N_7$ represent the first nitridosilicates containing a divalent rare earth metal.

The structure of $Eu_2Si_5N_8$ is based on a network of corner-sharing SiN_4 tetrahedra and is isotypic with $Sr_2Si_5N_8$ and $Ba_2Si_5N_8$ (Schlieper, Milius & Schnick, 1995). In this network half of the N atoms connect two, and the other half three, Si atoms. The $N^{[3]}$ atoms are arranged in corrugated sheets perpendicular to [100] (Fig. 1). The Eu^{2+} ions, which are mainly coordinated by $N^{[2]}$ atoms (Eu—N: 2.60–3.25 Å), are situated in channels along [100] formed by Si_6N_6 rings.

The Si–N network structure in $EuYbSi_4N_7$ is built up from star-shaped $[N(SiN_3)_4]$ building blocks (Fig. 2),

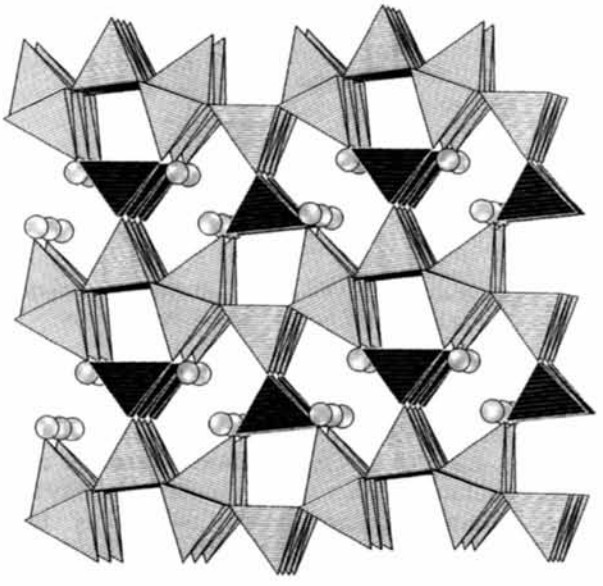

Fig. 1. Crystal structure of $Eu_2Si_5N_8$, viewed along [100].